

Annual Review of Physical Chemistry

Photochemistry of Organic Retinal Prostheses

Giovanni Manfredi,¹ Elisabetta Colombo,²
Jonathan Barsotti,¹ Fabio Benfenati,^{2,3}
and Guglielmo Lanzani^{1,4}

¹Center for Nano Science and Technology, Istituto Italiano di Tecnologia, 20133 Milan, Italy; email: giovanni.manfredi@iit.it, guglielmo.lanzani@iit.it

²Center for Synaptic Neuroscience and Technology, Istituto Italiano di Tecnologia, 16132 Genoa, Italy; email: elisabetta.colombo@iit.it, fabio.benfenati@iit.it

³Department of Experimental Medicine, University of Genoa, 16132 Genoa, Italy

⁴Department of Physics, Politecnico di Milano, 20133 Milan, Italy

Annu. Rev. Phys. Chem. 2019. 70:99–121

The *Annual Review of Physical Chemistry* is online at
physchem.annualreviews.org

<https://doi.org/10.1146/annurev-physchem-042018-052445>

Copyright © 2019 by Annual Reviews.
All rights reserved

**ANNUAL
REVIEWS CONNECT**

www.annualreviews.org

- Download figures
- Navigate cited references
- Keyword search
- Explore related articles
- Share via email or social media

Keywords

bioelectronics, photostimulation, polymer, retinal prostheses, light sensitivity recovery, organic optoelectronics

Abstract

Organic devices are attracting considerable attention as prostheses for the recovery of retinal light sensitivity lost to retinal degenerative disease. The biotic/abiotic interface created when light-sensitive polymers and living tissues are placed in contact allows excitation of a response in blind laboratory rats exposed to visual stimuli. Although polymer retinal prostheses have proved to be efficient, their working mechanism is far from being fully understood. In this review article, we discuss the results of the studies conducted on these kinds of polymer devices and compare them with the data found in the literature for inorganic retinal prostheses, where the working mechanisms are better comprehended. This comparison, which tries to set some reference values and figures of merit, is intended for use as a starting point to determine the direction for further investigation.

INTRODUCTION

Retinal prostheses are a family of devices that can be implanted in the eye to help people with the recovery of retinal light sensitivity lost to pathologies that degrade the functioning of photoreceptors in the retina. The vast majority of devices are based on inorganic semiconductor chips that create electrical stimuli (currents) upon the absorption of photons or the input supplied by an external visor. Such prostheses are well known, well investigated, and in some cases, commercially available (1–10). In **Figure 1**, we report the three major devices currently under study and development. Patients wearing such devices experience limited improvement of their condition, typically acquiring some light sensitivity and the ability to distinguish large, simple objects under strong illumination. In addition, this technology suffers from a number of shortcomings, such as limited biocompatibility, inability to cover extended areas of the retina, and local heat production (11). Moreover, most of the inorganic devices are based on the capacitive coupling of photodiode arrays with the retinal tissue and rely on well-known phenomena ruling the functioning of

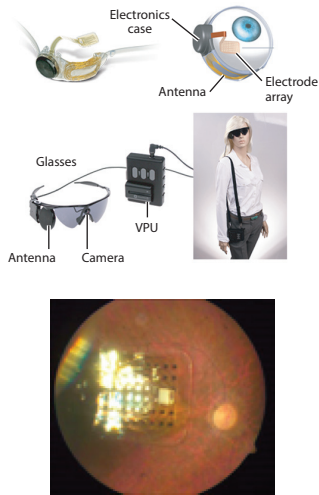
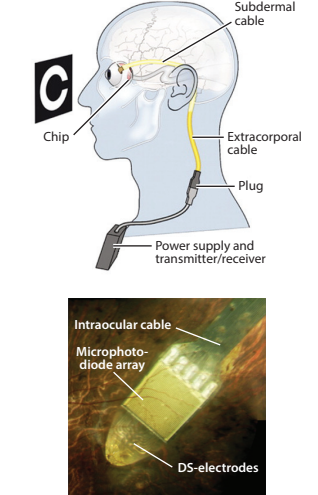
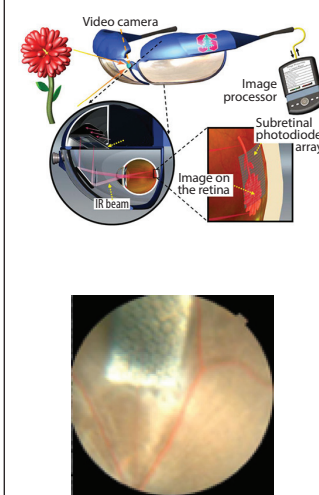
	ARGUS II (Second Sight)	ALPHA IMS (Retina Implant AG)	PRIMA (Pixium)
			
Silicon-made	✓	✓	✓
pixels/mm ²	2.5	160	200
Power cables	✓	✓	Wireless
External camera	✓	✗	✓
Approval	CE + FDA	CE	Not yet approved

Figure 1

The three major retinal prostheses currently under development and their main characteristics: Argus II (Second Sight), Alpha IMS (Retina Implant AG), and Prima (Pixium). Abbreviations: CE, Conformité Européene; DS, DropSens; FDA, US Food and Drug Administration; IR, infrared; LCD, liquid crystal display; VPU, vision processing unit. Argus II images are adapted with permission from <http://www.2-sight.com/system-overview-en.html>. Alpha IMS images adapted from Zrenner et al. (68), CC-BY 4.0. Prima images adapted with permission from Mathieson et al. (12).

inorganic optoelectronics on one side and extracellular neuronal stimulation on the other, as we report below.

Recently, the possibility of using radically different devices based on organic semiconductors has started to be investigated (13–18). In particular, Maya-Vetencourt et al. (13) proved that a sub-retinal implanted device based on a thin film of poly(3-hexylthiophene-2,5-diyl) (P3HT) successfully recovered vision in a genetic rat model of retinitis pigmentosa. The prosthesis is formed by a conformable planar substrate over which two polymer layers are deposited, the first composed of poly(3, 4-ethylenedioxythiophene)–polystyrene sulfonic acid (PEDOT:PSS) and the second of P3HT (**Figure 2c**). As P3HT is well known as a prototypical material for photovoltaics and many optoelectronic applications (19, 20), such a device resembles an organic photovoltaic cell in which one electrode is replaced by the extracellular electrolytic solution. Moreover, this polymer is biocompatible, as demonstrated by the successful growth of several different kinds of cells on its surface (21–23). It has a π – π^* optical gap in the green spectral region and a broad absorption spectral line shape, typically peaked at approximately 520 nm and spanning approximately 100 nm. In the retina application, the P3HT film is placed in the subretinal space, in contact with bipolar cells and other neurons of the inner retina. Upon light absorption, the polymer-generated signal is transferred to the cells. The experimental evidence shows that this coupling is effective in recovering a physiological response to light at retinal level that properly translates into visually evoked signals in the primary visual cortex.

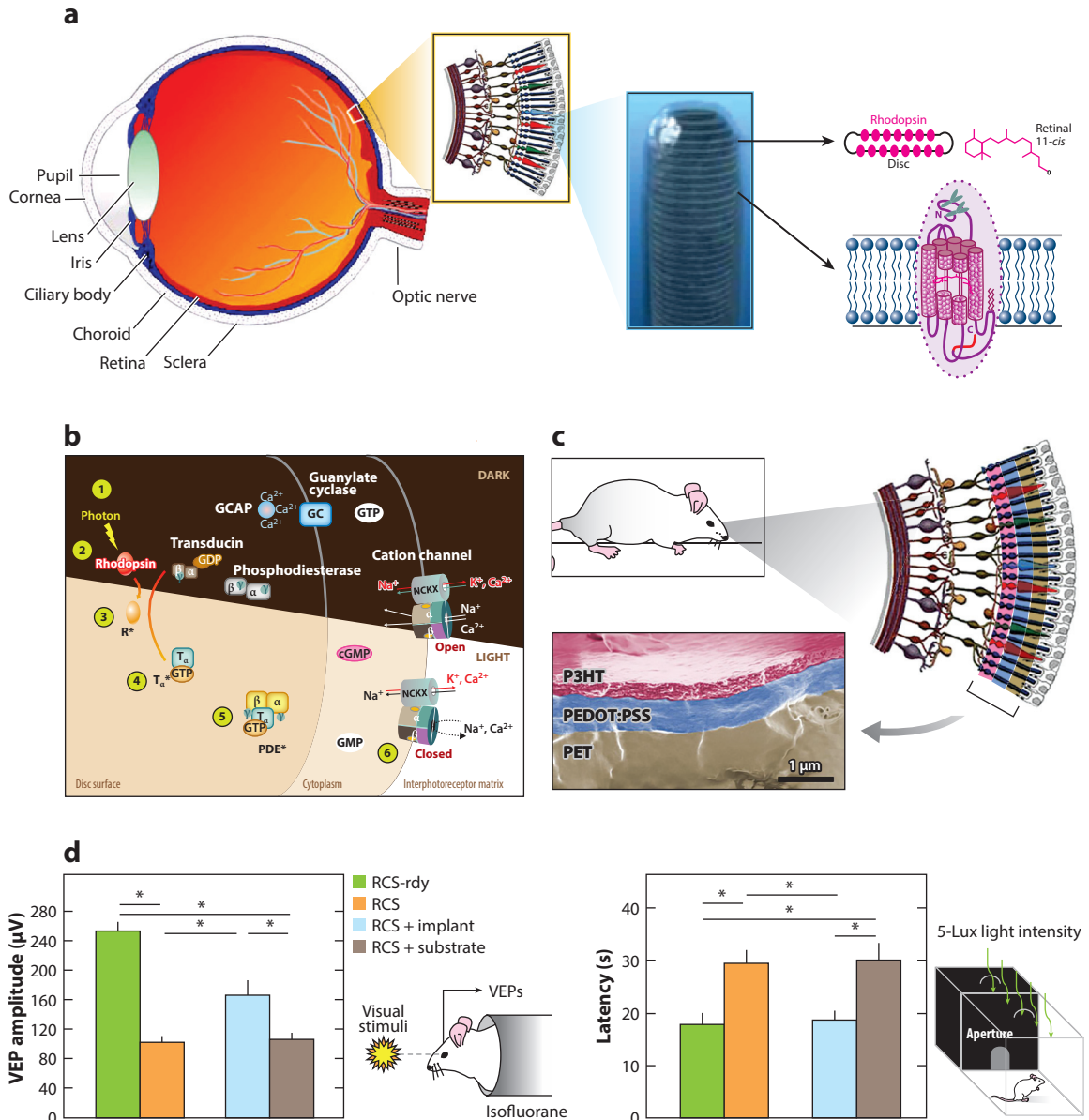
This exciting application opens up many questions on the actual working mechanism of the prosthesis and, more generally, on the kind of interaction that the organic semiconductor establishes at the biotic/abiotic interface. To explore this mechanism from a chemical-physical point of view, the characterization of the polymer films has been carried out in a biomimetic environment, and the biotic/abiotic interface has been reproduced in vitro by interfacing the polymeric films with human embryonic kidney (HEK-) 293 cells, astrocytes, or primary neurons. The picture that is emerging is quite complex, and there is no simple model that can capture all the observed features. Nevertheless, due to increased interest in the topic, a number of phenomena are now reasonably well understood. In this review, we provide a picture of the state of the art in organic-based biointerfaces, focusing on the possibilities of light-mediated coupling mechanisms.

We start with a brief description of the retina and implantation strategies of retinal prostheses. Since a retinal prosthesis is immersed in an aqueous environment, we then report on the photoexcitation scenario of P3HT immersed in saline solution and discuss the results of studies in which live cells are placed in contact with polymer devices. In addition, we briefly discuss the development and mechanistic understanding of organic retinal prostheses. Finally, we compare the data with figures of merit to determine a possible interpretation of the in vivo results.

THE RETINA AND DEVICE POSITIONING

The retina is a thin, multilayer structure located in the back of the eye and sandwiched between the pigment epithelium and the vitreous chamber (**Figure 2a**). The final goal of this tiny and yet amazing structure is to transduce light to biochemical signals that are preprocessed before being delivered to the optic nerve, which connects the retina to the brain, where images are formed and perceived. Contrary to the intuitive geometry that any light-detector has, light travels through three main layers of highly specialized neurons, tightly entangled with each other and packed with synaptic connections, before reaching the place where light transduction occurs. Photoreceptors are the cells responsible for the transduction of light into a chemical signal through a cascade of processes initiated by the photoisomerization of photochromic molecules embedded inside specialized proteins (opsins) (24). The entire process begins in the outer layer of the retina,

where opsins and chromophores are bound to the cell membranes of the photoreceptors' outer segments. In the dark, sodium channels in the photoreceptor membrane are constitutively open, maintaining the cell in a depolarized state that induces a continuous outflow of glutamate (the main excitatory neurotransmitter involved in retinal activity) from the photoreceptor terminal (pedicle). Upon absorption of a photon, the chromophore (retinal) isomerizes from 11-*cis* to all-*trans* form, triggering conformational changes in the rhodopsin molecule that contains it. The ensuing transduction cascade comprises various intermediaries, such as proteins and enzymes (**Figure 2b**),



(Caption appears on following page)

Figure 2 (Figure appears on preceding page)

Eye structure and current in-vivo results of organic retinal prostheses. (*a, left*) Schematic drawing of the eye and its principal components. (*right*) A 3D picture of a rod and a schematic diagram of rhodopsin in the outer segment discs. (*b*) Activation of rhodopsin by light and the phototransduction cascade. Light transduces the visual pigment via the following enzyme cascade: (●) photons, (●) rhodopsin, (●) activated rhodopsin (R^*) (metarhodopsin II), (●) a GTP binding protein (T_{α}^*) (transducin), (●) an enzyme hydrolyzing cGMP [cGMP-phosphodiesterase (PDE*)], and (●) closing of a membrane-bound cGMP-gated cation channel. (*c*) Study of the light response of an animal implanted with organic prostheses. (*top*) Schematic drawing of the positioning of the prostheses in subretinal configuration and (*bottom*) SEM cross sectional false-color image of a prosthesis. (*d, left*) Mean values of VEPs in response to flash stimuli (20 cd/m^2 ; 100 ms) and (*right*) mean values of latency in light-dark box test for different groups of rats: control rats (RCS-rdy; *green*), degenerated rats (RCS; *orange*), degenerated rats implanted with retinal prostheses (*light blue*), and rats implanted with the inert substrate (*light brown*). Abbreviations: P3HT, poly(3-hexylthiophene-2,5-diyl); PEDOT:PSS, poly(3, 4-ethylenedioxythiophene)-polystyrene sulfonic acid; PET, polyethylene terephthalate; RCS, Royal College of Surgeons; rdy, retinal dystrophy; VEP, visual evoked potential. Panels *a* and *b* are adapted from Kolb (24), CC-BY-NC 4.0. Panel *c* is adapted with permission from Maya-Vetencourt et al. (13), Antognazza et al. (16), and Kolb (24), CC-BY-NC 4.0. Panel *d* is adapted with permission from Maya-Vetencourt et al. (13).

eventually inducing closing of sodium channels, hyperpolarization of the photoreceptor cell, and light-dependent inhibition of glutamate release to the inner layers of the retina. Daily, photoreceptor disks are recycled and renewed thanks to the pigment epithelium, strategically located just outside the photoreceptor layer.

The modulation of glutamate release at the photoreceptor pedicle, in turn, affects the electrophysiological state of the postsynaptic bipolar cells. Such cells connect to the ganglion cells, which perform the last step of retinal processing and send trains of action potentials to the brain through the optic nerve. While crossing the retina, the coding of the light-generated signals is supported by horizontal and amacrine cells, other highly specialized interneurons interconnecting the photoreceptor, bipolar cell, and ganglion cell layers. This preprocessing of the visual signal by the inner retinal cells is very important for the design and interfacing of retinal prostheses.

Retinal prosthetics faces two main challenges, namely, an efficient and spatially resolved stimulation of the retinal tissue, and an effective processing of the light-generated signals before transduction to the optic nerve. A good coupling of any capacitive stimulation device in contact with the retinal tissue is paramount to achieve a sensitive improvement in visual signal transmission. However, the absence of photoreceptor signaling caused by inherited retinal dystrophy can lead to progressive degeneration and rewiring of the inner retina circuitry, thus interfering with the natural processing of any signal fed to the optic nerve. Accordingly, the retinal prosthetics community engineered three distinct strategies to achieve a good balance between high efficiency of stimulation and signal processing: suprachoroidal, epiretinal, and subretinal configurations (7).

In the suprachoroidal configuration, the prosthesis is placed on the outer part of the choroid, distant from the retina. This kind of device works by stimulating the retina across other tissues and needs very simple surgical interventions. However, the distance from retinal neurons poses limits to the necessary currents and to the precision of the stimulation that can be achieved, which can lead to scarce visual acuity. In the epiretinal configuration, the prosthesis is placed in the innermost part of the retina, in contact with the ganglion cell layers and the axon bundles forming the optic nerve. This configuration allows the use of very small currents to elicit neuronal responses but has the drawback of excluding the inner retinal circuitry for signal processing. As a side effect, patients implanted with an epiretinal prosthesis do not sense light as they were used to doing and need to adapt to a new way of perceiving visual stimuli. Lastly, in the subretinal configuration, the prosthesis is placed in the outer retina between the residues of degenerated photoreceptors and the choroid. The artificial apparatus directly stimulates bipolar cells, substituting *de facto* the photoreceptors. In this configuration, the visual system maintains its physiological pathway, reducing the need for novel algorithms of image processing at the cortical level and eventually

generating a more natural visual perception for the patient. However, the positioning of a device in subretinal configuration requires a more complex surgical intervention than in epiretinal or suprachoroidal configurations, because of an increased risk of retinal detachment.

The subretinal configuration is also used for organic prostheses tested on Royal College of Surgeons (RCS) rats affected by retinitis pigmentosa, a degenerative retinal disease that causes peripheral vision loss and eventually total blindness (13). In this case, the device is implanted via sclerotomy, and the semiconductive polymer is positioned in contact with the photoreceptor layer in the close proximity of bipolar cells (**Figure 2c**). Maya-Vetencourt et al. (13) showed that RCS rats implanted with the organic prosthesis recover most of their light sensitivity and visual acuity; in comparison to nonimplanted or sham-implanted animals, the electrical response detected at cortical level upon light stimulation (**Figure 2d, left**) in implanted rats greatly improves, and their behavioral responses to light become comparable to those of healthy rats (**Figure 2d, right**).

POLY(3-HEXYLTHIOPHENE-2,5-DIYL) PHOTOPHYSICS

Polymer semiconductors are large carbon-conjugated molecules that grant electron delocalization over their backbone. Electron delocalization shrinks the band gap and shifts the energy of the optical gap in the visible range. Moreover, these molecules have very large absorption cross-sections and can have high emission quantum yields. Semiconductor polymers can support electrical current thanks to the facilitated charge transfer reactions that occur in solid state. However, due to the hopping nature of the transport process, charge carrier mobility rarely exceeds $1 \text{ cm}^2/(\text{V}\cdot\text{s})$, several orders of magnitude lower than that observed in inorganic semiconductors (25–27). Conductivity is intrinsically very low, but it can be enhanced by chemical doping, as with inorganic semiconductors. These properties open up a number of possible applications, such as transistors, LEDs, and photovoltaic cells. The photophysical scenario, relevant to photonic and optoelectronic applications, is that of large organic molecules. Photoexcitation in solution generates singlet states that might convert to triplet states by intersystem crossing or deactivation back to ground state by internal conversion or radiative decay (28–30). Upon aggregation, intermolecular (interchain) phenomena kick in, for example, the generation of excitons in ordered phases or their separation into charge pairs (from charge transfer states to polaron pairs and even free carriers) (28, 29). Separation into charge pairs can be highly enhanced, virtually to unity quantum yield, by blending donor and acceptor moieties.

Although p- and n-type organic materials have been used (17), regioregular poly(3-hexylthiophene-2,5-diyl) (RR-P3HT) is currently the most studied material for organic retinal prostheses and the only one successfully employed in *in vivo* experiments so far (13–15, 21, 22). This polymer is a prototypical material that is soluble in common organic solvents and forms good quality films. Retinal prostheses made of P3HT show optical absorption across the visible range (**Figure 3a**) due to the inhomogeneously broadened vibronic absorption spectrum. As a practical consequence, the working spectral range of P3HT prostheses substantially overlaps that which the human eye can see (**Figure 3b**), spanning from approximately 400 to 700 nm.

Photoexcitation of P3HT in solid state generates singlet states or singlet excitons that decay back to the ground state both radiatively and nonradiatively, and a small fraction (<10%) of long-lived charged pairs (polarons). Polaron pairs are formed quickly during singlet spectral migration within the disordered phase (27) or by interchain coupling in lamellar structures (27, 28). In both cases, charge generation occurs in less than 1 ps. Oxygen reduction may, however, occur during the whole singlet lifetime, within approximately 1 ns. Continuous wavelength photoinduced absorption of P3HT films (depicted in **Figure 3c**) shows the spectroscopic signatures of polarons in P3HT and suggests a negligible population of triplet states. The absence of the triplet state is

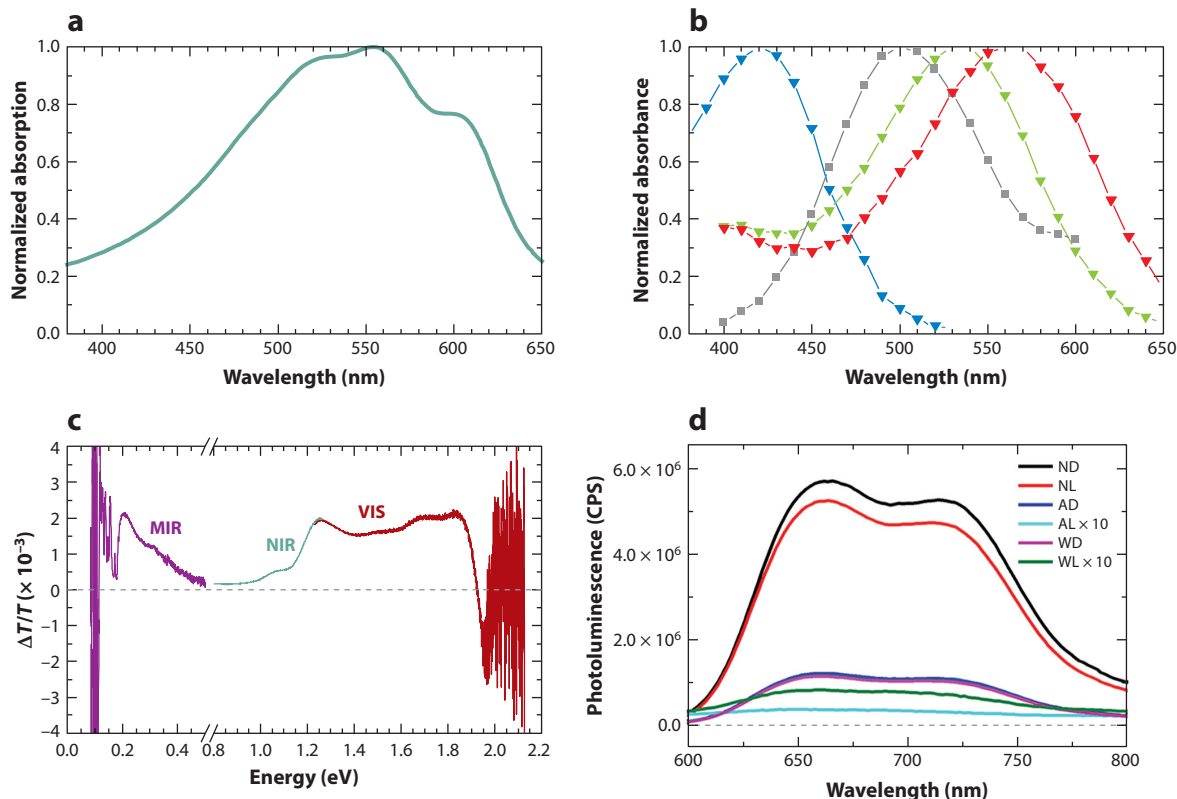


Figure 3

Optical properties of organic retinal prostheses. (a) Absorption spectrum of a typical regioregular poly(3-hexylthiophene-2,5-diyl) (RR-P3HT) spin-coated film. (b) Spectral responsivities of the natural photoreceptors: short wavelength-, medium wavelength-, and long wavelength-sensitive cones (blue, green, and red lines and triangles, respectively) and rods (gray line and squares). (c) Photoinduced absorption spectrum of a P3HT spin-coated film showing mid-infrared (MIR; black), near-infrared (NIR; green), and visible (VIS; red) spectra. (d) Photoluminescence spectra of P3HT samples exposed to different environmental conditions: stored in dark conditions and in controlled atmosphere [nitrogen dark (ND); black line] or upon air [air dark (AD) dark blue line]; illuminated continuously with visible light in nitrogen [nitrogen light (NL); red line] or in air [air light (AL); light blue line]; and exposed to direct contact with water in dark conditions [water dark (WD); magenta line] or in light conditions [water light (WL); green line]. Abbreviation: CPS, counts per second. Data in panel b is from Bowmaker & Dartnall (31). Panel c is courtesy of Elena Zucchetti. Panel d is adapted with permission from Bellani et al. (35); copyright 2018 American Chemical Society.

desirable in bioapplications, as triplets may interact with molecular oxygen to form singlet oxygen, a well-known cell killer. In the presence of oxygen doping or contamination, photoluminescence becomes quenched. Such behavior has been observed in P3HT films exposed to a controlled environment (Figure 3d) and is well characterized. The cause is an efficient energy transfer from the singlet excited state to the polaron state and a consequent internal conversion of the excited polaron state. This process occurs due to electron transfer to acceptors, such as oxygen, when doping is elevated and contributes to reducing the excited state lifetime from nano- to picoseconds. The long-lived fraction of the photoexcited population, up to milliseconds, is composed by relatively free holes and trapped electrons. In retinal prostheses, an electrode [typically indium tin oxide (ITO) or PEDOT:PSS] is deposited on the substrate, below the P3HT film. The interface between the electrode and the polymer provides a way to efficiently separate the charges in

excitons, thus increasing the number of long-lived species in the bilayer structure. Moreover, the electrode can also collect the charges generated in the semiconductor, slowing recombination.

In bioapplications, the P3HT layer is in contact with proteins and cell membranes that are immersed in the extracellular medium. This has led to investigation of the hybrid solid/liquid interface of a polymer with water and electrolytes as a first approximation of the biotic/abiotic interface (14, 21–23, 32).

A P3HT film in contact with water or an electrolyte behaves as a *p*-doped semiconductor by virtue of the strong electron affinity and energy matching of the penetrated hydrated oxygen (33–35). At equilibrium, due to polarization of the water molecules at the surface, the orbital energy approaching the interface gets reduced, mimicking band bending (35). The polarization of water molecules is consistent with an effective positive charge in the electrolyte close to the polymer surface and a negative charge inside the polymer (depletion region). The phenomenon is only formally equivalent to a semiconductor metal interface, since polymers do not have extended band states and, as stated above, the involved charge carrier mobility is much smaller. The watery dipole layer at the polymer surface participates in the formation of the Stern layer, together with ions in solution (Helmholtz layer). In addition, it was shown that the polymer surface changes its affinity for water, becoming less hydrophobic (in H₂O and under illumination, the contact angle drops below 90°) (35). However, it should be kept in mind that the surface boundary is not well defined and the interface is dispersed on several tens of nanometers due to ions, protons, and water penetration. Doping concentrations up to 10¹⁸ cm⁻³ in the soaked P3HT polymer layer have been observed in electrochemical cells by the Mott-Schottky plot technique. According to this scenario, upon photoexcitation, negative charges tend to migrate to the surface, causing a local ionic readjustment in the electrolyte.

LIGHT-INDUCED MODULATION OF CELL ACTIVITY

The photovoltaic properties of semiconducting polymers in contact with neurons have been well investigated thanks to the easy fabrication of stimulation devices and their intrinsic flexibility and proven biocompatibility. However, a thorough investigation of the nature of the interaction between these semiconducting interfaces and neuronal membranes is still lacking.

In fact, most of studies have limited their characterization to the ability of such compounds to favor growth and differentiation of cell lines and neurons (36–39). Stimulation of neuronal cells has relied on the assumption of a pure electrical or photovoltaic effect (14, 40). Within this framework, the application of photostimulation devices based on conjugated polymers as the basis of flexible retinal prosthetics has proven to be a potential powerful alternative to inorganic devices.

One of the most common electrophysiological techniques to record the spontaneous or stimulated electrical activity of excitable cells is patch-clamp. The possible characterizations offered by such a technique range from insights into the channel composition of a single-cell membrane to the study of electrical activity and interconnections at the tissue level. In particular, a whole-cell patch-clamp is performed with a micrometric glass capillary containing an Ag/AgCl electrode that is filled with intracellular-like solution and electrically sealed ($R > 1 \text{ G}\Omega$) to the cell bilipid layer. Eventually, the patched cell membrane is broken open, allowing electrochemical continuity between the cytosol and the Ag/AgCl, which signal is recorded versus a reference electrode positioned in the extracellular medium. Providing preferential electrochemical access to the cytosol, clamping either the current flowing through the membrane or the voltage across it, this versatile technique allows the study of ionic currents across a cell membrane in addition to its conductance, capacitance, and neuronal excitability properties (i.e., action potential firing). The first proof of principle for light-induced modulation of neuronal activity by means of a light-sensitive polymer

made use of the donor-acceptor blend RR-P3HT:PCBM on ITO (41). Ghezzi et al. (41) assessed the stability of the photocurrent generated by the polymer blend in a physiological solution and then confirmed the viability and the stability of electrophysiological properties of primary hippocampal neurons grown on the organic device. At this point, whole-cell patch-clamp recordings were performed on the same neurons upon spatially localized light stimulation. The application of 50-ms light pulses at 10 mW/mm² successfully generated action potentials in the neurons in contact with the polymeric compound. Interestingly, a close relation was found between the location of the stimulus relative to the cell soma and the action potential generation, confirming the spatial selectivity of the stimulation method.

Recently, a foldable, organic photovoltaic epiretinal prosthesis on a polydimethylsiloxane substrate was reported (18), consisting of a standard multilayered organic solar-cell structure based on a P3HT:PCBM blend, sandwiched between PEDOT:PSS and Ti as the anode and cathode, respectively. The POLYRETINA, composed of more than 2,000 pixels, proved to photostimulate blind retina explants in a mouse model of retinal degeneration well below the ANSI/ISO (American National Standards Institute/International Organization for Standardization) standards for retinal damage upon light exposure. Notwithstanding the potential of such a foldable solution, the photostimulation relies on the capacitive coupling between the metal cathode and the cell membranes, avoiding direct contact of the conjugated polymers with cells and tissues. Similarly, Gautam et al. (42) proposed a polymeric bulk heterojunction of P3HT:N2200 spin-coated on TiN electrodes as an epiretinal device, able to elicit light-sensitive responses in embryonic, blind chick retinas layered directly on top of the polymeric surface.

In photovoltaic applications, the most efficient organic solar cells attain unity internal quantum efficiency by exploiting the electron donor-acceptor interaction in the bulk. However, bulk properties may not play a crucial role when these materials are in direct contact with the biological environment. Indeed, we suspect that such biohybrid devices may have functional mechanisms that differ from those of conventional solar cells. Based on the conjecture that the interface is playing the crucial role, and that neuronal modulation is mediated by the capacitive charging of the polymer-electrolyte interface upon illumination, we tested a simpler active layer, constituted by P3HT only; it turned out that this efficiently produced photostimulation of cultured primary neurons and restored light sensitivity in explanted degenerate retinas using illumination power densities far below those used in AM1.5 conditions (15). Accordingly, a neuronal interface based on only P3HT on a flexible silk fibroin substrate has been implanted in wild-type rodents to investigate either the immune reaction or the stability of the device after a long exposure to the subretinal space (16). Indeed, immunostaining of astroglial and microglial markers in cryosections of implanted retinas dissected at various times after surgery showed that the unavoidable tissue reaction to the surgical implant was limited to the areas directly affected by the surgery and displayed a complete regression after 5 months. Most importantly, the tissue reaction to surgery did not alter the persistence and the properties of an intact polymeric layer structure. The same device was also reported to actively rescue in vivo more than 60% of light sensitivity and 95% of visual acuity in a rat model of retinal dystrophy up to 180 days after implantation (13). These reports clearly validate the potential of these materials to realize reliable all-organic, photo-neural stimulation devices for clinical applications. Further engineering of such devices is, however, limited by the incomplete understanding of the mechanisms underlying phototransduction. To investigate such phenomena in depth, characterizations have been performed in *in vitro* and *ex vivo* models.

A first report took advantage of nonexcitable HEK-293 cells grown on either P3HT or blends of P3HT and [6,6]phenyl-C61-butyric-acid-methyl ester (PCBM) to measure the modulation of the membrane potential by whole-cell current-clamp recordings under short pulses (20–200 ms) of light stimulation (**Figure 4a**). The photosensitive films on ITO or glass, together with the

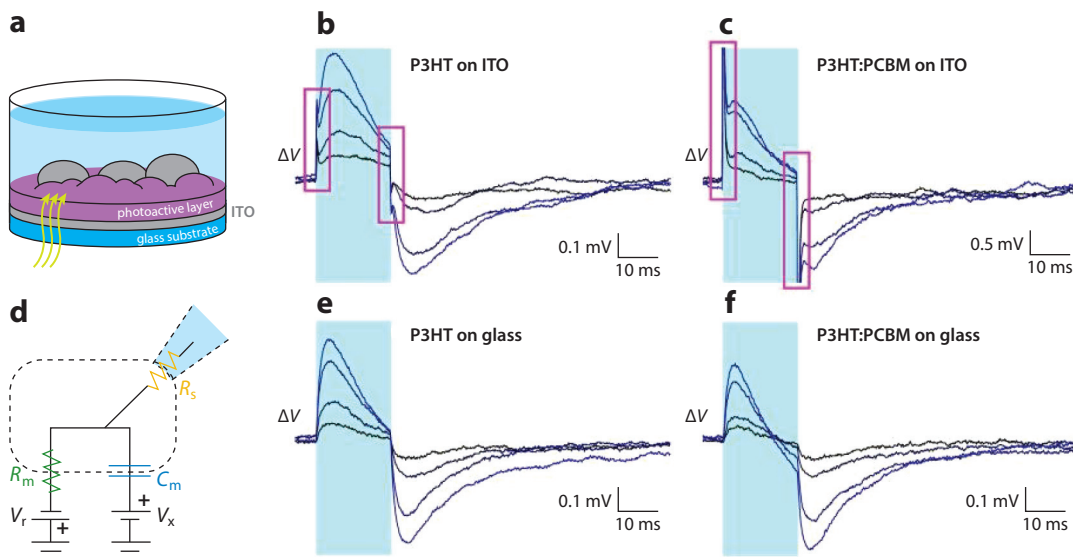


Figure 4

Human embryonic kidney (HEK-) 293 cell response to photostimulation on different substrates. (a) Experimental configuration used to study interaction between a polymer device and HEK cells. The photoactive layers are spin-coated thin films of poly(3-hexylthiophene-2,5-diyl) (P3HT) or a blend of P3HT and [6,6]phenyl-C61-butyric-acid-methyl ester (PCBM). The substrate is a glass coverslip, in some cases covered with a conductive indium tin oxide (ITO) layer. (d) Equivalent circuit representation of a cell membrane in a patch-clamp measurement. R_m and C_m are the membrane resistance (that includes the effect of all HEK-293 ion channels) and capacitance, respectively; R_s the series resistance of the patch; V_r the reversal potential; and V_x a term needed to take into account the asymmetries between inner and outer membrane surface charges and ion distributions. Membrane potential variation is measured in HEK-293 cells cultured on different photoactive substrates under pulsed illumination. Samples on ITO are (b) P3HT and (c) P3HT:PCBM, and samples on bare glass are (e) P3HT and (f) P3HT:PCBM. The traces in each panel refer to four increasing light intensities: 7.7 mW/mm², 15 mW/mm², 35 mW/mm², and 47 mW/mm². Light pulse duration (light blue shaded areas) is 20 ms. Each trace is the mean of 25 consecutive sweeps. All panels are adapted from Martino et al. (21), CC-BY 4.0.

employment of high-intensity illumination (4–60 mW/mm²), showed two concurring mechanisms: a capacitive charging of the polymer/electrolyte interface and a local heating of the polymer (21). The latter caused an early depolarization followed by a late hyperpolarization due to modulation of both membrane capacitance and conductance (Figure 4b,c). The fast photovoltage spike appeared at the light onset and offset and only in the presence of the ITO electrode, with amplitude proportional to the applied light intensity (Figure 4e,f). In fact, the photoinduced heating of the surface did not require the presence of the conductive electrode. This is easily accounted for by the underlying mechanism, as heating is due only to the nonradiative recombination of the photogenerated states. The temperature rise of the P3HT surface upon illumination, measured using a calibrated patch-clamp pipette, was found to be up to 7°C for a light intensity of 57 mW/mm², scaling linearly with light intensity and having typical rise and saturation times on the order of 10 ms and a few hundred milliseconds, respectively. Upon illumination, the cell soma touching the polymer surface is overrun by the temperature field, which is constant on the cell size. Figure 4d shows the equivalent circuit of the cleft between a device and the cell membrane, where R_m and C_m represent the membrane resistance and capacitance, respectively. The membrane resistance is related to the permeability to ions and depends on the density and properties of ion channels on the membrane and upon the equilibrium potential between the inside and the outside of the cell according to the Goldman-Hodgkin-Katz equation (43). The capacitance, instead, is mainly

related to the membrane surface, thickness, and dielectrical constant. By carrying out a careful evaluation of the experimental conditions, it was found that the K⁺ channels are responsible for a reduction of the membrane resistance with increasing temperature (44). The capacitance, instead, increases with temperature (45). This change may at first appear puzzling, as temperature rise is usually associated with expansion, hence the capacitance (*C*) reduction according to the simple planar capacitor equation:

$$\frac{dC}{C} = \frac{d\varepsilon}{\varepsilon} + \frac{dA}{A} - \frac{dl}{l},$$

where ε is the dielectrical function, *A* the surface, and *l* the thickness of the membrane. Indeed, the opposite is observed, and the most likely interpretation is a partial readjustment of the phospholipid chains in the membrane, perhaps the precursor of a phase transition (46, 47).

A further characterization of the thermal effect on the modulation of the neuronal signal by P3HT-related interfaces has been carried out in primary hippocampal neurons, and more intact and complex neuronal networks such as those of blind retinal explants and acute brain slices (44). Prolonged stimulation (500-ms pulses at 10–30 mW/mm²) induced silencing of the physiological firing during light stimulation of the neurons in the different preparations, followed by a rebound hyperactivity after light offset. Moreover, approximately 50% of the hyperpolarization amplitude induced by light was mediated by endogenous K⁺ conductance. However, the light-induced temperature rise in retinal prosthetics must be below 1°C, as coded in ocular safety regulations, which translates into strict limitations of the light power densities allowed for photostimulation. While the temperature effect is well established and documented, it is clear that other mechanisms should be at work under much lower intensities of illumination, such as those used in the *in vivo* experiments.

Further investigations of the photomodulation of neuronal activity by organic semiconductor interfaces revealed the presence of concurrent phenomena in addition to capacitive coupling and thermal heating, for example, the local acidification and/or hyperosmolarity of the illuminated area. Lodola et al. (22) employed HEK-293 cells stably transfected with Vanilloid Receptor 1 Transient Receptor Potential (TRPV1), which is responsible for body temperature regulation, response to pain, and synaptic plasticity, to mention just a few. TRPV1 can be activated by numerous factors, such as pH, heat, chemical/physical stimulation, and voltage. Most typical activation protocols rely on the application of extracellular capsaicin or temperature increases up to 43°C. In this study, while photothermal heating of the P3HT interface was confirmed (21), the presence of TRPV1 allowed the authors to obtain information on the generation of the light-evoked HEK-293T membrane potential changes. The recorded signal from HEK-293T was characterized by an early and fast depolarizing phase (approximately 48 ms at the maximum intensity), followed by an even stronger and slower light-dependent depolarization that was specifically induced by the presence of TRPV1, and that overcame completely the hyperpolarization observed in HEK-293 cells. Moreover, a careful analysis of the temperature evolution in the proximity of the illuminated interface revealed that heating alone cannot account for the TRPV1 activation, given that the temperature threshold was not reached even at the highest light intensity. The activation of the TRPV1 receptors has been explained by a sensitization of the channels due to an acidification of the extracellular space (48–50). In fact, a dependence of the depolarizing current upon the extracellular pH was recorded on the same cells exposed to light, showing that lower signals correspond to higher pH conditions. Thus, it has been proposed that the accumulation of electrons at the illuminated polymer surface induced an accumulation of positive ions, contributing to the channel

activation due to a local acidification. The concomitant acidosis and heat generation would ensure the activation of TRPV1 channels that causes membrane depolarization.

The potential involvement of a light-evoked acidification on the modulation of membrane activity has also been invoked on astrocytes (23). Astrocytes plated on P3HT:PCBM/ITO films strongly depolarize in response to light stimulation (**Figure 5a**). Voltage-clamp recordings on astrocytes plated on these supports showed an increase and decrease in membrane conductance at negative and positive potentials, respectively. The nature of the inward current elicited upon

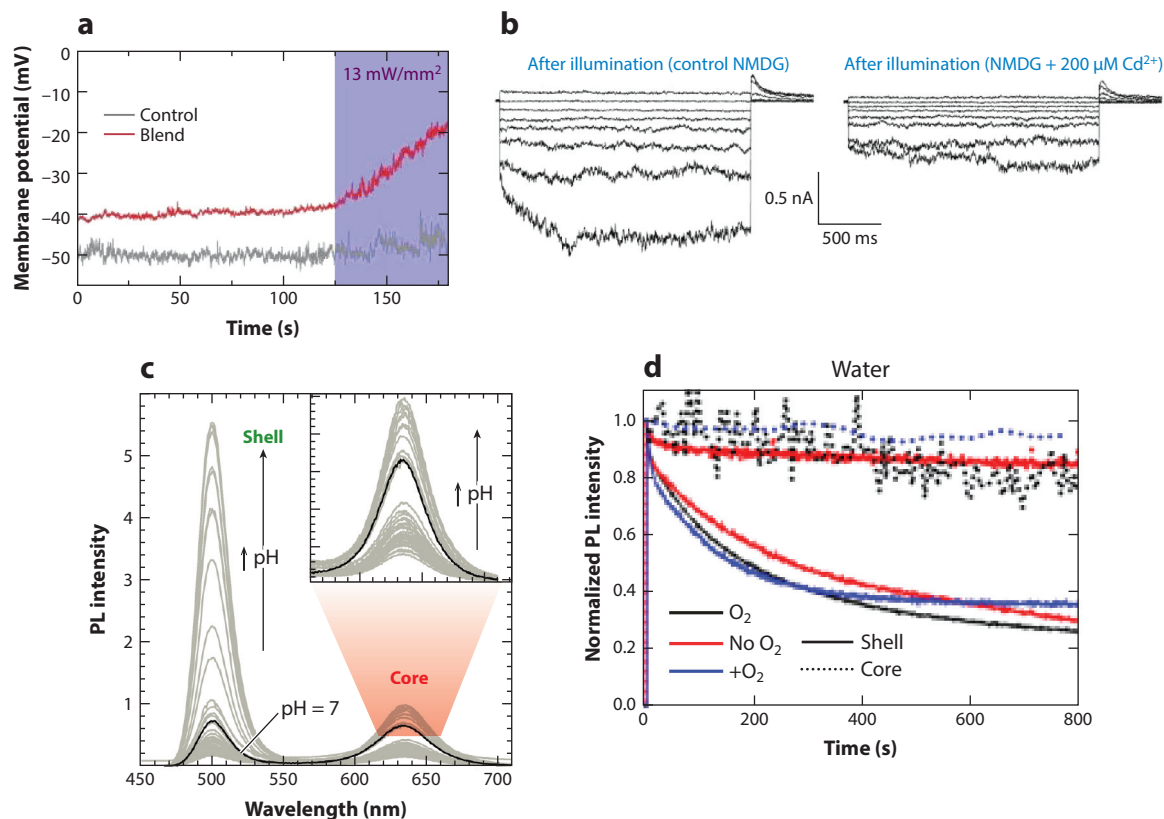


Figure 5

Astrocyte response to retinal prostheses and surface acidification. (a) Membrane potential measured in current-clamp mode recorded in astrocytes plated on PDL/P3HT-PCBM/ITO (red) and on PDL/ITO (gray). Light excitation is represented by the light purple bar; the power density is 13 mW/mm^2 . (b) Representative current traces evoked in astrocytes plated on P3HT-PCBM/ITO with a family of voltage steps from a V_h of 0 mV in 20-mV increments, from -120 to 20 mV. The traces have been recorded with intracellular CsCl and extracellular NMDG-Cl to isolate chloride conductance, photostimulating with a 561-nm laser (light density 13 mW/mm^2) before (left) and after (right) extracellular superfusion of submillimolar concentrations ($200 \times 10^{-6} \text{ M}$) of Cd^{2+} . This ion is a well-known Cl channel blocker. (c) PL of water-soluble CdSe/CdS DiB NCs at different pH values used as a pH probe. The NCs were excited at 405 nm (excitation fluence $1 \mu\text{J/cm}^2$). The pH was changed by adding stepwise 2–20 μL of HCl or NaOH (0.1 M). (d) PL intensity of shell (solid lines) and core (dotted lines) emissions of CdSe/CdS DiB NCs on P3HT measured in deionized water containing oxygen in equilibrium with standard atmosphere (black lines), in deoxygenated deionized water (red lines), and in oxygen-rich water (blue lines). Abbreviations: DiB, dot-in-bulk; ITO, indium tin oxide; NMDG, *N*-methyl-D-glucamine; NC, nanocrystal; P3HT, poly(3-hexylthiophene-2,5-diyl); PCBM, [6,6]phenyl-C61-butyric-acid-methyl ester; PDL, poly-D-lysine; PL, photoluminescence. Panels a and b are adapted with permission from Benfenati et al. (23). Panel c is adapted with permission from Bruni et al. (56). Panel d is adapted with permission from Mosconi et al. (55).

illumination relied on the activation of Cl^- conductance, as supported by voltage-clamp measurements performed after application of Cd^{2+} , which is known to inhibit ClC -mediated currents (51) (**Figure 5b**). The activation of these inwardly rectifying ClC -2 conductances upon illumination has been attributed to acidification at the polymer interface (52). Given the concomitant decrease in K^+ conductance while the light stimulation density increases, this transduction mechanism is supported by the evidence that the activity of the K_V channel family is modulated by extracellular pH (53, 54). Finally, the hypothesis of local acidification has been explored by using local probes at the polymer surface, for example, CdSe/CdS nanocrystals featuring ratiometric pH sensing upon prolonged illumination where deposited on the P3HT surface immersed in an aqueous solution (55, 56). In these systems, the photoluminescence efficiency is reduced as the pH decreases (**Figure 5c**), due to a specific electron transfer interaction occurring at the nanocrystal surface that modulates the effect of recombination traps. **Figure 5d** depicts how photoluminescence, and hence pH, decreases upon illumination. This further substantiates the conjecture that upon photoexcitation at the surface of P3HT, there is a change in the local ion concentration toward an electron-poor environment that could be sensed by the cell membrane. This is potentially a very important mechanism in neurons that express acid-sensing ion channels that respond to extracellular acidification with an inward current that depolarizes the membrane potential (57).

Other information on the biotic/abiotic interface and the potential role of polymer photoexcitation in biological photomodulation comes from P3HT nanoparticles (NPs) in water dispersions (58). NPs have been tested to evaluate their potential as injectable phototransducers for neuronal stimulation. In addition, in NPs the role of the surface is highlighted with respect to that of the bulk. The uptake and biocompatibility of the colloidal solutions have been assessed in HEK-293 cells, showing a diffuse localization in the cytoplasm, but not in the nuclei, and above all no side effects of cell exposure to the NPs (59). Based on the previous characterizations, P3HT photostimulation effects seem to rely on the interaction between the polymer and the cell membrane. For this reason and given the abovementioned study on cell uptake, P3HT NPs have been functionalized with amine-reactive *N*-hydroxysuccinimidyl ester groups, showing a preferential docking at the cell membranes with respect to the nonfunctionalized NPs (60). Similar to previous results on P3HT films (21), current-clamp recordings on HEK-293 cells exposed to the functionalized NPs showed the possibility of modulating membrane voltages upon illumination, an effect that was absent when NPs were internalized. The stimulation timing, light power densities employed, and aggregation degree of the NPs when in contact with saline solution support the idea of a photostimulation mediated by a localized heating of the membrane. P3HT NPs were revealed to be an interesting tool for the photomediated stimulation of neural tissues not only *in vitro* but also *in vivo*, according to a recent report dealing with hydras, eyeless freshwater polyps (61). The animals were exposed to P3HT NPs for up to 15 days with no adverse effects on their viability, while behavioral contraction studies showed an acquired light sensitivity in the animals exposed to the polymeric NPs. Moreover, the gained photosensitivity was also confirmed by a significant upregulation of gene families linked to various light transduction pathways, heat response, and oxidative stress.

POSSIBLE COUPLING MECHANISMS BETWEEN P3HT AND CELLS

As mentioned above, polymeric retinal prostheses successfully recovered visual function in rats with retinal dystrophy. We have evidence of four possible mechanisms responsible for the photostimulation of cell membrane activity induced by P3HT: thermal, faradaic, capacitive, and photochemical. Each one stems from a peculiar feature of the photophysical scenario. The thermal

process consists of a temperature rise near cell membranes upon energy absorption and dissipation into molecular vibrations. The faradaic mechanism is due to current injection into the cell following charge photogeneration at the interface and usually requires a current path to a counter electrode. In this review, we do not consider the electrochemical division of faradaic processes into capacitive and noncapacitive. In fact, both types arise from the passage of electrons across a polymer/electrolyte interface, although they present some differences. In capacitive faradaic (also referred to as pseudocapacitive) processes, the induced charge accumulation at the interface has a linear voltage dependence and is typically generated by very fast and reversible electrochemical processes involving delocalized charge states at the interface. In noncapacitive faradaic (also referred to as battery-like) processes, the induced charge accumulation has a nonlinear voltage dependence. The nonlinearity is usually explained by redox sites associated with highly localized and noninteracting electronic states at the interface. Here, slow and irreversible electrochemical reactions take place, generating a noncapacitive faradaic current that sums up to the capacitive faradaic contribution determining the total faradaic current. Accordingly, the photoexcitation outcome should be a charged population that lives long enough to establish a current across the cleft (typically tens of milliseconds).

The capacitive mechanism we refer to in this review is still induced by charge photogeneration, but the charge is accumulated at the polymer/electrolyte interface, where there are no transfer processes. Here, the charged layer changes the local osmolarity and pH of the electrolyte, perturbing the plasma membrane equilibrium.

In the photochemical mechanism, the excited states generated by light, again most likely the charged states, can take part in specific chemical reactions at the surface, reducing species in solution, such as oxygen, and giving rise to photochemical processes. Superoxide can form and quickly react with the environment, leading to a variety of reactive oxygen species (ROS). These specific photochemical products play a role in many metabolic processes, acting as messengers at low concentrations though becoming toxic at high concentrations.

To screen among the above-reported phenomena, it is necessary to refer to a standard situation. Indeed, all of the *in vitro/ex vivo* experiments were conducted under light conditions that are very different from the light that naturally enters the eye. Since our goal is to develop effective prostheses for the recovery of retinal light sensitivity, we should at least aim to achieve vision under common situations like an illuminated office, that is, with illumination intensities between 200 and 500 lx. Although in a real-world situation this would be white light illumination, for the sake of simplicity, we will suppose that the light is monochromatic with a wavelength of 555 nm. We can then assume that 1 lm is 1/683 W. A surface of 1 m² that diffuses isotropically in space at a 1-m distance from the eye would excite an area of the retina of 484 mm² with approximately 25 mW/cm². Alternatively, we can consider a point source of light of 1 cd as reference. Seen by the eye through a pupillary aperture 4 mm in diameter, it corresponds to 2×10^{-8} W. The point source is focused by the lens onto an area of the retina of approximately 4×10^{-5} cm², giving rise to an intensity of 0.5 mW/cm². Based on such numbers, and considering the large uncertainty of the estimate, which varies considerably with experimental conditions, we arbitrarily choose the value of 1 mW/cm² as our reference illumination intensity to understand the possible effects occurring in retinal prostheses.

Thermal Effect

To obtain a photothermal effect, various light actuators have been investigated, including metal and semiconductor NPs (62–66). In general, strong absorption and full nonradiative dissipation are the requirements for an efficient photothermal effect. The highest temperature change

available is in any case limited by the intensity of the exciting light. A power of 1 mW/cm^2 can only produce a very tiny increase in the local temperature, far below 1° (21). The corresponding change in membrane potential due to the thermal effect as described above is accordingly negligible and cannot account for the observed in vivo stimulation of blind retinas.

Faradaic Coupling

Faradaic coupling occurs when a device is able to supply enough current to elicit a response in a cell. The approach dates back to the eighteenth century when LeRoy reported the creation of light sensation in blind subjects upon their exposure to electrical currents (7). A retinal prosthesis that works upon Faradaic coupling is composed of two electrodes. One must be in close proximity to the retina and form an electrochemical junction with the physiological saline. The other electrode is needed to close the circuit and can either be near the first one or at a more distant position. The injection of charge in the saline is obtained by redox reactions that occur at the interface with the electrodes and requires the right alignment of energy bands of the electrode material. Typical reactions that occur are oxidation and reduction of water or electron transfer from and to polyvalent ions (67). The current flows through retinal tissues and induces a local redistribution of the ionic charges on cell membranes. If a certain depolarization threshold is reached for neurons, then an action potential is fired. Two types of current can be used to elicit a response: cathodic or anodic current. In the cathodic configuration, negative charges are injected and the potential in the proximity of the electrode is reduced, depolarizing the cell membrane. Farther from the electrode, positive ions are attracted to compensate for the change in potential, and the membrane becomes effectively hyperpolarized. Conversely, anodic currents hyperpolarize the proximal cells and depolarize those farther away. Since both types of injection cause depolarization, they can be used to stimulate the retina; however, the required anodic currents are typically 3–7 times higher than the respective cathodic currents (7).

The direct injection of currents inside retinal tissues has been quite well investigated (8, 68–76). The injection of current through tissues may have undesired effects that can undermine health and safety in clinical applications, such as Joule heating of the tissue due to carrier drift, which would also contribute to the heating effect previously discussed, or the generation of redox reaction products that are potentially harmful to the biological environment. Moreover, if such reactions are nonreversible, repeated stimuli can result in the accumulation of these harmful species, and a prolonged use of a Faradaic prosthesis may become problematic. To avoid such drawbacks and reverse the redox reactions occurring at the interfaces, one can perform biphasic stimulations, in which each stimulus is divided into a positive and negative current (7, 77).

In 2011, Zrenner et al. (68) showed that in patients implanted with a 4×4 array of $100 \times 100 \text{ }\mu\text{m}^2$ TiN electrodes in subretinal position, the minimum charge transfer needed to elicit a visual stimulus was between 20 and 60 nC delivered in 0.5- to 6-ms intervals. We can take these values as a reference to estimate whether the Faradaic current that can be hypothetically created by a passive subretinal device is sufficient to elicit a visual stimulus. Indeed, the minimum current needed by the reported values is $40 \text{ }\mu\text{A}$.

Considering a monochromatic light beam with photon energy $h\nu = 2 \text{ eV}$ and an intensity of 1 mW/cm^2 impinging on an area $A = 100 \times 100 \text{ }\mu\text{m}^2$ and being fully absorbed, the maximum electron current that can be created is $I_0 = 5 \text{ }\mu\text{A}$. This occurs only if the quantum conversion efficiency of photons to charges equals unity. If we consider a time interval of 20 ms, the amount of charge generated by the pixel of area A is $q = 100 \text{ nC}$, which is well above the minimum threshold of 20 nC previously reported. However, this occurs only in the case of total conversion of photons to charges. In organic semiconductors, the internal quantum efficiency is typically between 10^{-4}

and 10^{-2} and the charge that can be created is on the order of 0.01–1 nC, not enough to elicit an electrical response in the retinal tissues. Thus, it is clear that photocurrent injection cannot represent the only mechanism triggering retina stimulation by organic semiconductors and that additional mechanisms at the biotic/abiotic interface are involved.

Capacitive Coupling

Capacitive coupling is another form of electrical coupling that can occur between a device and retinal tissues and has been nicely investigated by Fromherz and colleagues (70, 72, 78–81) in both single neurons and explanted retinas. This interaction occurs when no current is directly injected into the biological tissue and no reaction occurs at the saline-electrode interface. In this case, the electrical field in the tissue is modified by the device that induces a local potential variation. In principle, this alone could be responsible for a response in the cells, but other effects may also occur. Indeed, the accumulation of positive or negative charges at the surface of one electrode could attract counterions in the aqueous solutions to reestablish the neutrality. Such attraction locally modifies the acidity of the solution by reducing or increasing the pH and/or the osmolarity (55, 82) and can, in principle, induce a change in cell membrane permeability to ions or modify neurotransmission by eliciting a physiological response (83–87).

It is interesting to compare the values reported for organic devices with those reported for silicon by Eickenscheidt et al. (81). The authors evaluated the response of rabbit retinas to the stimulation induced by a silicon device working as a capacitor. The device was able to create an electrical field by accumulating charge with very low leakages. They studied the rheobase (i.e., the minimum current needed to elicit an action potential in neurons) and chronaxie (i.e., the time needed to elicit an action potential using a current double the rheobase) necessary to elicit a response in subretinal configuration for both cathodic and anodic stimulations. In both cases, the necessary charge threshold was below $10 \mu\text{C}/\text{cm}^2$. Hypothetically, using a passive optodevice and considering a monochromatic exciting light of $10 \text{ mW}/\text{mm}^2$ (10^3 times higher than the standard situation we defined above and corresponding to full-daylight illumination), one should be able to accumulate $10^4 \mu\text{C}/\text{cm}^2$ in 20 ms, generating a sufficient electrical field to elicit a response. However, this would be true only in the case of a perfect absorption and no-loss hypothesis. We know that the quantum efficiency of photon-to-charge conversion is very low and the threshold value of $10 \mu\text{C}/\text{cm}^2$ may not be reachable. The current state of the art concerning the creation of a strong capacitive charge in organic devices can be found in a paper by Głowacki and colleagues (17). There, they report that proper illumination induces a cathodic surface potential of approximately -25 mV , measured $10 \mu\text{m}$ from the device surface. They also calculated the charge accumulated by the device exploiting a reference TiN multielectrode array and found a capacitive charge of more than $100 \mu\text{C}/\text{cm}^2$, well above the threshold reported by Fromherz and colleagues (70, 72, 78–81). The values reported by Głowacki's group also suggest that other non-state-of-the-art devices, like those reported by Lanzani's group (13, 58), could in principle have enough surface charge to elicit a response in retinal tissues to strong light excitation. Such non-state-of-the-art devices, proven efficient in rats (13), show anodic surface potentials on the order of some millivolts under stimulation by light on the order of tens of milliwatts per square millimeter. Exploiting the values reported by Głowacki and colleagues (17), one may estimate that the surface charge was between 20 and $100 \mu\text{C}/\text{cm}^2$, which is above the Fromherz limit and compatible with a reasonable photon-to-surface charge conversion efficiency of 10^{-3} (30, 88). Despite this observation, however, we have to consider that we are talking about very high power densities that exceed the normal light intensity that would hit the retina in a common office situation. Under the

latter conditions, one cannot reach the capacitive stimulation threshold suggested by Fromherz and colleagues. Thus, we tend to rule out that an electrostatic stimulus due to capacitive effect is the only cause of retinal stimulation and vision restoration *in vivo*.

Photochemistry

Currently, the vast majority of retinal prostheses are based on electrical interaction of devices with tissues. As we described above, polymer prostheses can potentially work through the formation of charges and capacitive coupling, if the light used has sufficiently high power densities. However, we cannot exclude that other phenomena occur, such as photochemical reactions at the interface between the prosthesis and the cell medium. The products of such reactions could in principle elicit cell membrane activity. A substantial indication that something more than capacitive may happen is also given by the results obtained on hydras using P3HT NPs (61). Indeed, in that case, no donor acceptor interface is present, and one cannot assume to have an efficient generation of electrical field.

From the literature, it is well known that P3HT under illumination can form ROS (88–93), even though the nature of these species and their role in the polymer photodegradation mechanism are still discussed (20, 90, 94–98). It is known that singlet oxygen is formed in P3HT, as are superoxide, hydroxyl radical, and hydrogen peroxide (89, 99–102). Such species suggest the use of P3HT as photocatalyst for water photolysis and hydrogen production. In biological applications, however, ROS pose a danger to cells due to oxidative stress, and concentrations above a certain threshold are toxic (103–110). Accordingly, much effort is spent on the study of the role of ROS in pathologies. However, such potentially harmful species are also naturally involved in healthy biological processes and in low concentrations can lead to positive effects (eustress) (103, 111–115).

To the best of our knowledge, no study has been conducted on the use of ROS to actively elicit a response in excitable cells. The oxygen species created by the prostheses could directly affect the membrane properties of cells by reversibly modifying the ionic conductivity of the membrane or interacting with enzymes and extracellular proteins. Also, neurotransmitter uptake and stability could be influenced by ROS. To estimate the concentrations involved, let us suppose that light hitting the retina possesses a power density of approximately 1 mW/cm^2 . Given a charge conversion efficiency of 10^{-3} , a retinal prosthesis could reasonably create a current between 0.1 and $1 \text{ }\mu\text{A/cm}^2$, that is, a current equivalent to the production of a number of electrons per second per square centimeter between 10^{15} and 10^{16} . If something relevant happens in an implanted retina, we suppose that it happens in close proximity to the device, for example, $<50 \text{ }\mu\text{m}$ from it. This limit has been greatly overestimated, and Ghezzi and colleagues (15) reported that P3HT devices were not able to elicit responses in explanted retinas if the distance from neurons surpassed $20 \text{ }\mu\text{m}$. Using this assumption, we can then identify a volume of 0.005 cm^3 in which chemical reactions may occur. Since we have no hint about the chemical reactions that may occur, we cannot extensively discuss all the possibilities. However, we can suppose that the electrons produced by the device are allowed to react with biomolecules in the retinal extracellular medium. The concentration of such species, for example, amino acids, is on the order of tens of micromolars (116). This means that the number of molecules in a volume of 0.005 cm^3 is roughly 10^{14} , which is below the number of electrons produced for that volume. If every electron can efficiently interact with extracellular molecules, then it could be possible, for example, to completely deplete specific messengers or inhibit the functioning of biomolecules with just some milliseconds of stimulus. Therefore, photoinitiated chemical reactions could in principle be an explanation for the stimulation of retinal tissues in contact with a polymer prosthesis.

CONCLUSIONS

To conclude, we have provided here an overview of the various approaches adopted for the development of polymeric retinal prostheses and of the in vitro and in vivo studies to understand their working principles. Among organic-based devices, only polymer (P3HT) planar prostheses have been successfully tested in vivo in animal models, but there is growing research activity in this field. Despite the practical interest in these devices, there is a lack of solid and comprehensive understanding of the working principles driving the hybrid interface. We have here considered various models in an effort to capture the essential mechanisms of coupling involved and to give a reference for further study of the distinct interactions that can occur at the interface with retinal neurons.

DISCLOSURE STATEMENT

The authors are not aware of any affiliations, memberships, funding, or financial holdings that might be perceived as affecting the objectivity of this review.

ACKNOWLEDGMENTS

The authors appreciate funding from the Italian Ministry of Health (project RF-2013-02358313) and Fondazione 13 Marzo (Parma, Italy).

LITERATURE CITED

1. Vaidya A, Borgonovi E, Taylor RS, Sahel J-A, Rizzo S, et al. 2014. The cost-effectiveness of the Argus II retinal prosthesis in retinitis pigmentosa patients. *BMC Ophthalmol.* 14:49
2. Rizzo S, Belting C, Cinelli L, Allegrini L, Genovesi-Ebert F, et al. 2014. The Argus II retinal prosthesis: 12-month outcomes from a single-study center. *Am. J. Ophthalmol.* 157:1282–90
3. Lorach H, Goetz G, Smith R, Lei X, Mandel Y, et al. 2015. Photovoltaic restoration of sight with high visual acuity. *Nat. Med.* 21:476–82
4. Lorach H, Goetz G, Mandel Y, Lei X, Kamins TI, et al. 2015. Performance of photovoltaic arrays in-vivo and characteristics of prosthetic vision in animals with retinal degeneration. *Vis. Res.* 111:142–48
5. Goetz G, Smith R, Lei X, Galambos L, Kamins T, et al. 2015. Contrast sensitivity with a subretinal prosthesis and implications for efficient delivery of visual information. *Investig. Ophthalmol. Vis. Sci.* 56:7186
6. Park JH, Shim S, Jeong J, Kim SJ. 2017. A multi-photodiode array-based retinal implant IC with on/off stimulation strategy to improve spatial resolution. *J. Semicond. Technol. Sci.* 17:35–41
7. Yue L, Weiland JD, Roska B, Humayun MS. 2016. Retinal stimulation strategies to restore vision: fundamentals and systems. *Prog. Retin. Eye Res.* 53:21–47
8. Weiland JD, Walston ST, Humayun MS. 2016. Electrical stimulation of the retina to produce artificial vision. *Annu. Rev. Vis. Sci.* 2:273–94
9. Lin T-C, Chang H-M, Hsu C-C, Hung K-H, Chen Y-T, et al. 2015. Retinal prostheses in degenerative retinal diseases. *J. Chin. Med. Assoc.* 78:501–5
10. Ayton LN, Blamey PJ, Guymer RH, Luu CD, Nayagam DAX, et al. 2014. First-in-human trial of a novel suprachoroidal retinal prosthesis. *PLOS ONE* 9:e115239
11. Benfenati F, Lanzani G. 2018. New technologies for developing second generation retinal prostheses. *Lab Anim.* 47:71–75
12. Mathieson K, Loudin J, Goetx G, Huie P, Wang L, et al. 2012. Photovoltaic retinal prosthesis with high pixel density. *Nat. Photonics* 6:391–97
13. Maya-Vetencourt JF, Ghezzi D, Antognazza MR, Colombo E, Mete M, et al. 2017. A fully organic retinal prosthesis restores vision in a rat model of degenerative blindness. *Nat. Mater.* 16:681–89

14. Martino N, Ghezzi D, Benfenati F, Lanzani G, Antognazza MR. 2013. Organic semiconductors for artificial vision. *J. Mater. Chem. B* 1:3768
15. Ghezzi D, Antognazza MR, Maccarone R, Bellani S, Lanzarini E, et al. 2013. A polymer optoelectronic interface restores light sensitivity in blind rat retinas. *Nat. Photonics* 7:400–6
16. Antognazza MR, Di Paolo M, Ghezzi D, Mete M, Di Marco S, et al. 2016. Characterization of a polymer-based, fully organic prosthesis for implantation into the subretinal space of the rat. *Adv. Healthcare Mater.* 5:2271–82
17. Rand D, Jakešová M, Lubin G, Věbraité I, David-Pur M, et al. 2018. Direct electrical neurostimulation with organic pigment photocapacitors. *Adv. Mater.* 30:1707292
18. Ferlauto L, Airaghi Leccardi MJI, Chenais NAL, Gilliéron SCA, Vagni P, et al. 2018. Design and validation of a foldable and photovoltaic wide-field epiretinal prosthesis. *Nat. Commun.* 9:992
19. Dang MT, Hirsch L, Wantz G. 2011. P3HT:PCBM, best seller in polymer photovoltaic research. *Adv. Mater.* 23:3597–602
20. Holliday S, Ashraf RS, Wadsworth A, Baran D, Yousaf SA, et al. 2016. High-efficiency and air-stable P3HT-based polymer solar cells with a new non-fullerene acceptor. *Nat. Commun.* 7:11585
21. Martino N, Feyen P, Porro M, Bossio C, Zucchetti E, et al. 2015. Photothermal cellular stimulation in functional bio-polymer interfaces. *Sci. Rep.* 5:8911
22. Lodola F, Martino N, Tullii G, Lanzani G, Antognazza MR. 2017. Conjugated polymers mediate effective activation of the Mammalian Ion Channel Transient Receptor Potential Vanilloid 1. *Sci. Rep.* 7:8477
23. Benfenati V, Martino N, Antognazza MR, Pistone A, Toffanin S, et al. 2014. Photostimulation of whole-cell conductance in primary rat neocortical astrocytes mediated by organic semiconducting thin films. *Adv. Healthcare Mater.* 3:392–99
24. Kolb H, Nelson R, Fernandez E, Jones B, ed. 2012. *Webvision: The Organization of the Retina and Visual System*. Salt Lake City: Univ. Utah Health Sci. Cent. <https://webvision.med.utah.edu/>
25. Fazzi D, Caironi M. 2015. Multi-length-scale relationships between the polymer molecular structure and charge transport: the case of poly-naphthalene diimide bithiophene. *Phys. Chem. Chem. Phys.* 17:8573–90
26. Choi HH, Rodionov YI, Paterson AF, Panidi J, Saranin D, et al. 2018. Accurate extraction of charge carrier mobility in 4-probe field-effect transistors. *Adv. Funct. Mater.* 28:1707105
27. Köhler A, Bässler H. 2015. *Electronic Processes in Organic Semiconductors: An Introduction*. Weinheim, Ger.: Wiley-VCH
28. Österbacka R, An CP, Jiang XM, Vardeny ZV. 2000. Two-dimensional electronic excitations in self-assembled conjugated polymer nanocrystals. *Science* 287:839
29. Korovyanko OJ, Österbacka R, Jiang XM, Vardeny ZV, Janssen RAJ. 2001. Photoexcitation dynamics in regioregular and regiorandom polythiophene films. *Phys. Rev. B* 64:235122
30. Lanzani G. 2012. *The Photophysics Behind Photovoltaics and Photonics*. Weinheim, Ger.: Wiley-VCH
31. Bowmaker JK, Dartnall HJA. 1980. Visual pigments of rods and cones in a human retina. *J. Physiol.* 298:501–11
32. Tullii G, Desii A, Bossio C, Bellani S, Colombo M, et al. 2017. Bimodal functioning of a mesoporous, light sensitive polymer/electrolyte interface. *Org. Electron.* 46:88–98
33. Schafferhans J, Baumann A, Wagenpfahl A, Deibel C, Dyakonov V. 2010. Oxygen doping of P3HT:PCBM blends: influence on trap states, charge carrier mobility and solar cell performance. *Org. Electron.* 11:1693–700
34. Guerrero A, Boix PP, Marchesi LF, Ripolles-Sanchis T, Pereira EC, Garcia-Belmonte G. 2012. Oxygen doping-induced photogeneration loss in P3HT:PCBM solar cells. *Sol. Energy Mater. Sol. Cells* 100:185–91
35. Bellani S, Fazzi D, Bruno P, Giussani E, Canesi EV, et al. 2014. Reversible P3HT/oxygen charge transfer complex identification in thin films exposed to direct contact with water. *J. Phys. Chem. C* 118:6291–99
36. Rowland DCL, Aquilina T, Klein A, Hakimi O, Alexis-Mouthuy P, et al. 2016. A comparative evaluation of the effect of polymer chemistry and fiber orientation on mesenchymal stem cell differentiation. *J. Biomed. Mater. Res. A* 104:2843–53

37. Liu X, Liu R, Cao B, Ye K, Li S, et al. 2016. Subcellular cell geometry on micropillars regulates stem cell differentiation. *Biomaterials* 111:27–39
38. Hsiao Y-S, Liao Y-H, Chen H-L, Chen P, Chen F-C. 2016. Organic photovoltaics and bioelectrodes providing electrical stimulation for PC12 cell differentiation and neurite outgrowth. *ACS Appl. Mater. Interfaces* 8:9275–84
39. Bonetti S, Pistone A, Brucalè M, Karges S, Favaretto L, et al. 2015. A lysinated thiophene-based semiconductor as a multifunctional neural bioorganic interface. *Adv. Healthc. Mater.* 4:1190–202
40. Abdullaeva OS, Schulz M, Balzer F, Parisi J, Lützen A, et al. 2016. Photoelectrical stimulation of neuronal cells by an organic semiconductor–electrolyte interface. *Langmuir* 32:8533–42
41. Ghezzi D, Antognazza MR, Dal Maschio M, Lanzarini E, Benfenati F, Lanzani G. 2011. A hybrid bioorganic interface for neuronal photoactivation. *Nat. Commun.* 2:166
42. Gautam V, Rand D, Hanein Y, Narayan KS. 2014. A polymer optoelectronic interface provides visual cues to a blind retina. *Adv. Mater.* 26:1751–56
43. Hodgkin AL, Katz B. 1949. The effect of sodium ions on the electrical activity of the giant axon of the squid. *J. Physiol.* 108:37–77
44. Feyen P, Colombo E, Endeman D, Nova M, Laudato L, et al. 2016. Light-evoked hyperpolarization and silencing of neurons by conjugated polymers. *Sci. Rep.* 6:22718
45. Shapiro MG, Homma K, Villarreal S, Richter C-P, Bezanilla F. 2012. Infrared light excites cells by changing their electrical capacitance. *Nat. Commun.* 3:736
46. Holl MMB. 2008. Cell plasma membranes and phase transitions. In *Phase Transitions in Cell Biology*, ed. GH Pollack, W-C Chin, pp. 171–81. Dordrecht, Neth.: Springer
47. Chapman D. 1975. Phase transitions and fluidity characteristics of lipids and cell membranes. *Q. Rev. Biophys.* 8:185
48. Ryu S, Liu B, Qin F. 2003. Low pH potentiates both capsaicin binding and channel gating of VR1 receptors. *J. Gen. Physiol.* 122:45–61
49. Hui K, Liu B, Qin F. 2003. Capsaicin activation of the pain receptor, VR1: multiple open states from both partial and full binding. *Biophys. J.* 84:2957–68
50. Reeh PW, Kress M. 2001. Molecular physiology of proton transduction in nociceptors. *Curr. Opin. Pharmacol.* 1:45–51
51. Ferroni S, Marchini C, Nobile M, Rapisarda C. 1997. Characterization of an inwardly rectifying chloride conductance expressed by cultured rat cortical astrocytes. *Glia* 21:217–27
52. Sharma A, Mathijssen SGJ, Kemerink M, de Leeuw DM, Bobbert PA. 2009. Proton migration mechanism for the instability of organic field-effect transistors. *Appl. Phys. Lett.* 95:253305
53. Fedida D, Zhang S, Kwan DCH, Eduljee C, Kehl SJ. 2005. Synergistic inhibition of the maximum conductance of Kv1.5 channels by extracellular K⁺ reduction and acidification. *Cell Biochem. Biophys.* 43:231–42
54. Cohen A, Ben-Abu Y, Hen S, Zilberberg N. 2008. A novel mechanism for human K2P2.1 channel gating. Facilitation of C-type gating by protonation of extracellular histidine residues. *J. Biol. Chem.* 283:19448–55
55. Mosconi E, Salvatori P, Saba MI, Mattoni A, Bellani S, et al. 2016. Surface polarization drives photoinduced charge separation at the P3HT/water interface. *ACS Energy Lett.* 1:454–63
56. Bruni F, Pedrini J, Bossio C, Santiago-Gonzalez B, Meinardi F, et al. 2017. Two-color emitting colloidal nanocrystals as single-particle ratiometric probes of intracellular pH. *Adv. Funct. Mater.* 27:1605533
57. Zeng W-Z, Liu D-S, Liu L, She L, Wu L-J, Xu T-L. 2015. Activation of acid-sensing ion channels by localized proton transient reveals their role in proton signaling. *Sci. Rep.* 5:14125
58. Di Maria F, Lodola F, Zucchetti E, Benfenati F, Lanzani G. 2018. The evolution of artificial light actuators in living systems: from planar to nanostructured interfaces. *Chem. Soc. Rev.* 47:4757–80
59. Zucchetti E, Zangoli M, Bargigia I, Bossio C, Di Maria F, et al. 2017. Poly(3-hexylthiophene) nanoparticles for biophotonics: study of the mutual interaction with living cells. *J. Mater. Chem. B* 5:565–74
60. Zangoli M, Di Maria F, Zucchetti E, Bossio C, Antognazza MR, et al. 2017. Engineering thiophene-based nanoparticles to induce phototransduction in live cells under illumination. *Nanoscale* 9:9202–9

61. Tortiglione C, Antognazza MR, Tino A, Bossio C, Marchesano V, et al. 2017. Semiconducting polymers are light nanotransducers in eyeless animals. *Sci. Adv.* 3:e1601699
62. Yang J, Choi J, Bang D, Kim E, Lim E-K, et al. 2011. Convertible organic nanoparticles for near-infrared photothermal ablation of cancer cells. *Angew. Chem. Int. Ed.* 50:441–44
63. O'Neal DP, Hirsch LR, Halas NJ, Payne JD, West JL. 2004. Photo-thermal tumor ablation in mice using near infrared-absorbing nanoparticles. *Cancer Lett.* 209:171–76
64. Lyu Y, Fang Y, Miao Q, Zhen X, Ding D, Pu K. 2016. Intraparticle molecular orbital engineering of semiconducting polymer nanoparticles as amplified theranostics for in vivo photoacoustic imaging and photothermal therapy. *ACS Nano* 10:4472–81
65. Zharov VP, Mercer KE, Galitovskaya EN, Smeltzer MS. 2006. Photothermal nanotherapeutics and nanodiagnostics for selective killing of bacteria targeted with gold nanoparticles. *Biophys. J.* 90:619–27
66. Jaque D, Martínez Maestro L, del Rosal B, Haro-Gonzalez P, Benayas A, et al. 2014. Nanoparticles for photothermal therapies. *Nanoscale* 6:9494–530
67. Merrill DR, Bikson M, Jefferys JGR. 2005. Electrical stimulation of excitable tissue: design of efficacious and safe protocols. *J. Neurosci. Methods* 141:171–98
68. Zrenner E, Bartz-Schmidt KU, Benav H, Besch D, Bruckmann A, et al. 2011. Subretinal electronic chips allow blind patients to read letters and combine them to words. *Proc. R. Soc. B* 278:1489–97
69. Sekirnjak C, Hottowy P, Sher A, Dabrowski W, Litke AM, Chichilnisky EJ. 2006. Electrical stimulation of mammalian retinal ganglion cells with multielectrode arrays. *J. Neurophysiol.* 95:3311–27
70. Fromherz P. 2005. The neuron-semiconductor interface. In *Bioelectron: Theory and Application*, ed. I Willner, E Katz, pp. 339–93. Weinheim, Ger.: Wiley-VCH
71. Gekeler F, Kobuch K, Schwahn HN, Stett A, Shinoda K, Zrenner E. 2004. Subretinal electrical stimulation of the rabbit retina with acutely implanted electrode arrays. *Graefes Arch. Clin. Exp. Ophthalmol.* 242:587–96
72. Fromherz P. 2002. Electrical interfacing of nerve cells and semiconductor chips. *ChemPhysChem* 3:276–84
73. Chow AY, Chow VY. 1997. Subretinal electrical stimulation of the rabbit retina. *Neurosci. Lett.* 225:13–16
74. Zrenner E. 2013. Fighting blindness with microelectronics. *Sci. Transl. Med.* 5:210ps16
75. Wilke R, Gabel V-P, Sachs H, Bartz Schmidt K-U, Gekeler F, et al. 2011. Spatial resolution and perception of patterns mediated by a subretinal 16-electrode array in patients blinded by hereditary retinal dystrophies. *Investig. Ophthalmol. Vis. Sci.* 52:5995
76. Rivnay J, Wang H, Fenno L, Deisseroth K, Malliaras GG. 2017. Next-generation probes, particles, and proteins for neural interfacing. *Sci. Adv.* 3:e1601649
77. Lilly JC, Hughes JR, Alvord EC, Galkin TW. 1955. Brief, noninjurious electric waveform for stimulation of the brain. *Science* 121:468–69
78. Vassanelli S, Fromherz P. 1999. Transistor probes local potassium conductances in the adhesion region of cultured rat hippocampal neurons. *J. Neurosci.* 19:6767–73
79. Schoen I, Fromherz P. 2007. The mechanism of extracellular stimulation of nerve cells on an electrolyte-oxide-semiconductor capacitor. *Biophys. J.* 92:1096–111
80. Fromherz P, Stett A. 1995. Silicon-neuron junction: capacitive stimulation of an individual neuron on a silicon chip. *Phys. Rev. Lett.* 75:1670–73
81. Eickenscheidt M, Jenkner M, Thewes R, Fromherz P, Zeck G. 2012. Electrical stimulation of retinal neurons in epiretinal and subretinal configuration using a multicapacitor array. *J. Neurophysiol.* 107:2742–55
82. Lounasvuori MM, Holt KB. 2017. Acid deprotonation driven by cation migration at biased graphene nanoflake electrodes. *Chem. Commun.* 53:2351–54
83. Tombaugh GC, Somjen GG. 1996. Effects of extracellular pH on voltage-gated Na⁺, K⁺ and Ca²⁺ currents in isolated rat CA1 neurons. *J. Physiol.* 493:719–32
84. Doering CJ, McRory JE. 2007. Effects of extracellular pH on neuronal calcium channel activation. *Neuroscience* 146:1032–43

85. Bray GE, Ying Z, Baillie LD, Zhai R, Mulligan SJ, Verge VMK. 2013. Extracellular pH and neuronal depolarization serve as dynamic switches to rapidly mobilize trkA to the membrane of adult sensory neurons. *J. Neurosci.* 33:8202–15
86. Sinning A, Hübner CA. 2013. Minireview: pH and synaptic transmission. *FEBS Lett.* 587:1923–28
87. Chen Z-L, Huang R-Q. 2014. Extracellular pH modulates GABAergic neurotransmission in rat hypothalamus. *Neuroscience* 271:64–76
88. Suppes G, Ballard E, Holdcroft S. 2013. Aqueous photocathode activity of regioregular poly(3-hexylthiophene). *Polym. Chem.* 4:5345
89. Floresyona D, Goubard F, Aubert P-H, Lampre I, Mathurin J, et al. 2017. Highly active poly(3-hexylthiophene) nanostructures for photocatalysis under solar light. *Appl. Catal. B* 209:23–32
90. Manceau M, Rivaton A, Gardette J-L. 2008. Involvement of singlet oxygen in the solid-state photochemistry of P3HT. *Macromol. Rapid Commun.* 29:1823–27
91. Muktha B, Madras G, Guru Row TN, Scherf U, Patil S. 2007. Conjugated polymers for photocatalysis. *J. Phys. Chem. B* 111:7994–98
92. Abdou MSA, Holdcroft S. 1995. Solid-state photochemistry of π -conjugated poly(3-alkylthiophenes). *Can. J. Chem.* 73:1893–901
93. Chen L, Mizukado J, Suzuki Y, Kutsuna S, Aoyama Y, et al. 2014. An ESR study on superoxide radical anion generation and its involvement in the photooxidative degradation of poly-3-hexylthiophene in chlorobenzene solution. *Chem. Phys. Lett.* 605–6:98–102
94. Seemann A, Sauermann T, Lungenschmied C, Armbruster O, Bauer S, et al. 2011. Reversible and irreversible degradation of organic solar cell performance by oxygen. *Sol. Energy* 85:1238–49
95. Hintz H, Peisert H, Egelhaaf H-J, Chassé T. 2011. Reversible and irreversible light-induced p-doping of P3HT by oxygen studied by photoelectron spectroscopy (XPS/UPS). *J. Phys. Chem. C* 115:13373–76
96. Manceau M, Rivaton A, Gardette J-L, Guillerez S, Lemaître N. 2009. The mechanism of photo- and thermooxidation of poly(3-hexylthiophene) (P3HT) reconsidered. *Polym. Degrad. Stab.* 94:898–907
97. Chen L, Yamane S, Mizukado J, Suzuki Y, Kutsuna S, et al. 2015. ESR study of singlet oxygen generation and its behavior during the photo-oxidation of P3HT in solution. *Chem. Phys. Lett.* 624:87–92
98. Aoyama Y, Yamanari T, Murakami TN, Nagamori T, Marumoto K, et al. 2015. Initial photooxidation mechanism leading to reactive radical formation of polythiophene derivatives. *Polym. J.* 47:26–30
99. Grysziel M, Sytnyk M, Jakešová M, Romanazzi G, Gabrielsson R, et al. 2018. General observation of photocatalytic oxygen reduction to hydrogen peroxide by organic semiconductor thin films and colloidal crystals. *ACS Appl. Mater. Interfaces* 10:13253–57
100. Watanabe M. 2017. Dye-sensitized photocatalyst for effective water splitting catalyst. *Sci. Technol. Adv. Mater.* 18:705–23
101. Fumagalli F, Bellani S, Schreier M, Leonardi S, Rojas HC, et al. 2016. Hybrid organic–inorganic H₂-evolving photocathodes: understanding the route towards high performance organic photoelectrochemical water splitting. *J. Mater. Chem. A* 4:2178–87
102. Bellani S, Ghadirzadeh A, Meda L, Savoini A, Tacca A, et al. 2015. Hybrid organic/inorganic nanostructures for highly sensitive photoelectrochemical detection of dissolved oxygen in aqueous media. *Adv. Funct. Mater.* 25:4531–38
103. Devasagayam T, Tilak J, Boloor K, Sane KS, Ghaskadbi SS. 2004. Free radicals and antioxidants in human health: current status and future prospects. *J. Assoc. Phys. India* 52:794–804
104. Wolff SP, Gamer A, Dean RT. 1986. Free radicals, lipids and protein degradation. *Trends Biochem. Sci.* 11:27–31
105. Valko M, Izakovic M, Mazur M, Rhodes CJ, Telser J. 2004. Role of oxygen radicals in DNA damage and cancer incidence. *Mol. Cell. Biochem.* 266:37–56
106. Halliwell B, Gutteridge JMC. 2015. *Free Radicals in Biology and Medicine*. Oxford, UK: Oxford Univ. Press. 5th ed.
107. Halliwell B, Gutteridge JMC. 1985. Oxygen radicals and the nervous system. *Trends Neurosci.* 8:22–26
108. Halliwell B, Gutteridge JMC. 1984. Oxygen toxicity, oxygen radicals, transition metals and disease. *Biochem. J.* 219:1–14

109. Dugan LL, Choi DW. 1994. Excitotoxicity, free radicals, and cell membrane changes. *Ann. Neurol.* 35:S17–21
110. Barrington P. 1988. Abnormal electrical activity induced by free radical generating systems in isolated cardiocytes. *J. Mol. Cell. Cardiol.* 20:1163–78
111. Schipper HM. 2004. Redox neurology: visions of an emerging subspecialty. *Ann. NY Acad. Sci.* 1012:342–55
112. Lander HM. 1997. An essential role for free radicals and derived species in signal transduction. *FASEB J.* 11:118–24
113. Dröge W. 2002. Free radicals in the physiological control of cell function. *Physiol. Rev.* 82:47–95
114. Afanas'ev IB. 2007. Signaling functions of free radicals superoxide & nitric oxide under physiological & pathological conditions. *Mol. Biotechnol.* 37:2–4
115. Sies H. 2017. Hydrogen peroxide as a central redox signaling molecule in physiological oxidative stress: oxidative eustress. *Redox Biol.* 11:613–19
116. Heinämäki AA, Muhonen ASH, Piha RS. 1986. Taurine and other free amino acids in the retina, vitreous, lens, iris/ciliary body, and cornea of the rat eye. *Neurochem. Res.* 11:535–42